

# Hypoxia-induced pulmonary hypertension and chronic lung disease: caveolin-1 dysfunction an important underlying feature

Jing Huang<sup>1</sup>, Maria Frid<sup>2</sup>, Michael H. Gewitz<sup>1</sup>, John T. Fallon<sup>3</sup>, Dale Brown<sup>2</sup>, Greta Krafsur<sup>2</sup>, Kurt Stenmark<sup>2</sup> and Rajamma Mathew<sup>1,4</sup>

<sup>1</sup>Department of Pediatrics, Maria Fareri Children's Hospital at Westchester Medical Center, New York Medical College, Valhalla, NY, USA; <sup>2</sup>Cardiovascular Pulmonary Research Laboratories, Departments of Pediatrics and Medicine, University of Colorado Anschutz Medical Campus, Aurora, CO, USA; <sup>3</sup>Department of Pathology, New York Medical College, Valhalla, NY, USA; <sup>4</sup>Department of Physiology, New York Medical College, Valhalla, NY, USA

## Abstract

Caveolin-1 (cav-1) has been shown to play a significant role in the pathogenesis of pulmonary hypertension (PH). In the monocrotaline model of PH, the loss of endothelial cav-1 as well as reciprocal activation of proliferative and anti-apoptotic pathways initiate the disease process and facilitate its progression. In order to examine the role of cav-1 in hypoxia-induced PH, we exposed rats and neonatal calves to hypobaric hypoxia and obtained hemodynamic data and assessed the expression of cav-1 and related proteins eNOS, HSP90, PTEN, gp130, PY-STAT3,  $\beta$ -catenin, and Glut1 in the lung tissue. Chronic hypoxic exposure in rats (48 h–4 weeks) and calves (two weeks) did not alter the expression of cav-1, HSP90, or eNOS. PTEN expression was significantly decreased accompanied by PY-STAT3 activation and increased expression of gp130, Glut1, and  $\beta$ -catenin in hypoxic animals. We also examined cav-1 expression in the lung sections from steers with chronic hypoxic disease (Brisket disease) and from patients with chronic lung disease who underwent lung biopsy for medical reasons. There was no cav-1 loss in Brisket disease. In chronic lung disease cases, endothelial cav-1 expression was present, albeit with less intense staining in some cases. In conclusion, hypoxia did not alter the cav-1 expression in experimental models. The presence of cav-1, however, did not suppress hypoxia-induced activation of PY-STAT3 and  $\beta$  catenin, increased gp130 and Glut1 expression, or prevent the PTEN loss, indicating cav-1 dysfunction in hypoxia-induced PH.

## Keywords

Glut1, PTEN,  $\beta$ -catenin

Date received: 18 September 2018; accepted: 22 February 2019

Pulmonary Circulation 2019; 9(1) 1–12

DOI: 10.1177/2045894019837876

## Introduction

Hypoxia plays an important role in pulmonary hypertension (PH). Acute hypoxia causes pulmonary arterial contraction and elevated pulmonary artery pressure (PAP), while sustained hypoxia results in pulmonary vascular remodeling, medial thickening, and extension of smooth muscle into partially muscular arteries.<sup>1</sup> Extrapulmonary arteries are reported to be stiff in hypoxic rats.<sup>2</sup> Furthermore, hypoxia has been shown to impair endothelium-dependent relaxation in rats and in rabbit pulmonary arteries in organ culture, whereas endothelium-denuded vessels responded

normally to nitroprusside,<sup>3,4</sup> indicating that hypoxia causes endothelial dysfunction, but the relaxation response of smooth muscle cells (SMC) is not affected. Similarly, endothelium-dependent relaxation is reported to be impaired in the pulmonary arteries of patients with chronic obstructive pulmonary disease (COPD), and endothelium-denuded vessels respond normally to nitroprusside.<sup>5,6</sup>

Corresponding author:

Rajamma Mathew, Room A11, Basic Science Building, New York Medical College, 15 Dana Road, Valhalla, NY 10595, USA.

Email: rajamma\_mathew@NYMC.edu



Creative Commons Non Commercial CC BY-NC: This article is distributed under the terms of the Creative Commons Attribution-NonCommercial 4.0 License (<http://www.creativecommons.org/licenses/by-nc/4.0/>) which permits non-commercial use, reproduction and distribution of the work without further permission provided the original work is attributed as specified on the SAGE and Open Access pages (<https://us.sagepub.com/en-us/nam/open-access-at-sage>).

© The Author(s) 2019.

Article reuse guidelines:  
[sagepub.com/journals-permissions](http://sagepub.com/journals-permissions)  
[journals.sagepub.com/home/pul](http://journals.sagepub.com/home/pul)



Recent studies indicate that caveolin-1 (cav-1) may have an important role in the pathogenesis of PH. Cav-1 is the major protein constituent of caveolae, a subset of specialized lipid rafts, found in a variety of cells including endothelial cells (EC), SMC, and epithelial cells. Cav-1 interacts with signaling molecules in caveolae, including eNOS through protein-protein interaction, and exerts negative regulation of the target proteins, through the cav-1 scaffolding domain (amino acids 82–101).<sup>7</sup> Significant loss of endothelial cav-1 has been reported in monocrotaline (MCT)-induced PH and in human pulmonary arterial hypertension (PAH).<sup>8,9</sup> However, during hypoxia, cav-1 has been shown to form a tight complex with eNOS and accompanying impaired intracellular Ca<sup>2+</sup> leads to the inhibition of endothelium-dependent relaxation.<sup>10</sup> Furthermore, hypoxia has a negative effect on store-operated and receptor-operated Ca<sup>2+</sup> channels leading to the inhibition of Ca<sup>2+</sup> entry, and introduction of cav-1 scaffolding protein rescues ATP-induced Ca<sup>2+</sup> entry in EC from chronic hypoxic pulmonary arteries.<sup>11</sup>

Progressive loss of endothelial cav-1 and reciprocal activation of proliferative pathways such as tyrosine (705) phosphorylated signal transduction and activator of transcription 3 (PY-STAT3) is observed in the lungs before the onset of PH in the MCT model.<sup>12</sup> Furthermore, persistent activation of PY-STAT3 has been reported in the pulmonary arterial EC from patients with idiopathic PAH.<sup>13</sup> Importantly, cav-1 has been shown to act as a suppressor of cytokine signaling and to inhibit PY-STAT3 activation.<sup>12,14</sup> At the transcriptional level, STAT3 is regulated by  $\beta$ -catenin, a key mediator of Wnt signaling pathway, and STAT3 activation increases nuclear accumulation of  $\beta$ -catenin, indicating a positive feedback loop. Dysregulation of the Wnt/ $\beta$ -catenin pathway has been linked to several forms of cancer; recent studies have shown increased expression of  $\beta$ -catenin in plexiform lesions in the lungs of patients with idiopathic PAH.<sup>15,16</sup> Interestingly, cav-1 inhibits  $\beta$ -catenin by sequestering it to the plasma membrane.<sup>17</sup>

Phosphatase and TENsin homolog deleted on chromosome 10 (PTEN), an onco-suppressor, with a dual specificity lipid and protein phosphatase, controls negatively the PI3K/AKT pathway which regulates cell growth and survival. Recent studies have shown that PTEN is dysregulated in both hypoxia and MCT-induced PH.<sup>18</sup> Fibroblasts from idiopathic pulmonary fibrosis lungs exhibit low cav-1 levels accompanied by low membrane PTEN levels; overexpression of cav-1 restores membrane PTEN levels, inhibits Akt phosphorylation, and suppresses cell proliferation. It is interesting to note that PTEN contains a cav-1 binding motif and, in part, co-localizes in caveolae.<sup>19,20</sup> Thus, cav-1 expression determines the membrane PTEN levels through its binding sequence. PTEN has also been shown to have an inverse relationship with  $\beta$ -catenin<sup>21</sup> and it negatively regulates STAT3 and its activation; importantly, membrane localization of PTEN is considered responsible for the inactivation of STAT3.<sup>22,23</sup> PTEN loss has been shown to

increase Glut1 expression on the plasma membrane and the ectopic expression of PTEN abolishes the expression of Glut1 via dephosphorylating AKT.<sup>24,25</sup> Not only is Glut1 present in the cav-1-rich plasma membrane, but cav-1 has also been shown to negatively correlate with Glut1 expression in the placenta of patients with gestational diabetes mellitus.<sup>26,27</sup> Thus, cav-1 and PTEN appear to have a close relationship and similar functions and participate in maintaining vascular homeostasis.

To test our hypothesis that cav-1 dysfunction has an important role in hypoxia-induced PH, we examined the time-dependent alterations in the expression of cav-1, eNOS, HSP90, PTEN, and related proteins, gp130, PY-STAT3,  $\beta$  catenin, and Glut1 during hypoxia in rats and neonatal calves. In addition, we examined lung sections from steers that died of chronic hypoxic PH (Brisket disease).<sup>28</sup> We also examined cav-1 expression in lung sections from patients with lung diseases who had undergone lung biopsy for medical reasons. Our findings support the idea that hypoxia does not per se alter cav-1 expression, but clearly contributes to its dysfunction as indicated by decreased PTEN expression and the activation of PY-STAT3.

## Materials and methods

Male Sprague-Dawley rats weighing 150–175 g were obtained from Charles River Laboratories (Wilmington, MA, USA). Rats were allowed to acclimatize in the animal facility for five days before the start of experimental protocols and had free access to laboratory chow and water. Protocols were approved by the Institutional Animal Care and Use Committee of New York Medical College and conform to the guiding principles for the use and care of laboratory animals of the American Physiological Society and the National Institutes of Health. Rats were subjected to hypobaric hypoxia (P<sub>B</sub> 380 mmHg) or room air for 48 h, one, two, and four weeks as per protocol. Rats were removed from hypobaric chamber twice a week for 15 min to clean the bedding and replenish the food and water, and to measure the body weight.

### Measurements of right ventricular systolic pressure (RVSP)

RVSP was measured using methods described previously.<sup>12</sup> Briefly, rats were anesthetized with an intraperitoneal injection of pentobarbital (60 mg/kg). Through an incision in the neck, the trachea was exposed and cannulated with PE240 tubing, and the rat ventilated in room air at a rate of approximately 70–80 breaths per minute with a tidal volume of 0.83 mL/100 g body weight. The chest was opened and PE50 tubing inserted into the right ventricle and the pressure was recorded on a Grass polygraph (model 7E). At the end of the pressure measurements, the lungs were perfused with autoclaved normal saline to remove blood. The right lung was removed, quickly frozen in liquid N<sub>2</sub>, and stored at

–80 °C for protein extraction. Heart and the left lung were placed in 10% buffered formaldehyde.

### Assessment of right ventricular hypertrophy (RVH)

A week later, the heart was removed from formaldehyde and atria trimmed. The free wall of the right ventricle (RV) was separated from the left ventricle and the septum (LV). The ratio of RV/LV was calculated to assess RVH.

### Bovine neonatal hypoxia and Brisket disease

Neonatal calves (age = 1–3 days, weight = 35–45 kg) were exposed to hypobaric hypoxia ( $P_B$  450 mmHg) for two weeks; hemodynamic data were obtained as previously described.<sup>29</sup> At the end of the procedure, the lung tissue was processed for western blot and embedded in paraffin for histological and immunofluorescence studies. In addition, lung sections were obtained from steers with Brisket disease for histological and immunofluorescence studies. Standard veterinary care was used following institutional guidelines in compliance with Institutional Animal Care and Use Committee-approved protocols at the Department of Physiology, School of Veterinary Medicine, Colorado State University (Fort Collins, CO, USA).

### Human chronic lung disease

We examined the expression of cav-1 in lung sections obtained from nine patients with various lung diseases who underwent lung biopsy for medical reasons. The study was approved by the Internal Review Board of New York Medical College. The age range was 17–71 years; there were five women and four men. These patients had lung diseases such as chronic obstructive pulmonary disease (COPD), emphysema, and spontaneous pneumothorax, and a few patients had associated co-morbidities. The control lung tissue was obtained from a woman aged 25–30 years who underwent lung biopsy for an unrelated cause.

**Patient 1.** A man aged 15–20 years with asthma and a history of recurrent pneumothorax was admitted with chest pain. He was diagnosed with left pneumothorax. During the surgical procedure a lung biopsy was obtained, which revealed focal bullous lesion, sub-pleural scarring, and intra-alveolar histiocytes.

**Patient 2.** A woman aged 15–20 years was treated for spontaneous pneumothorax. The lung biopsy revealed lung parenchyma with emphysematous bullae, pleural thickening associated with focal chronic inflammation, and medial thickening of the pulmonary artery.

**Patient 3.** Lung biopsy from a woman aged 31–40 years, treated for pneumothorax, revealed pleural fibrosis and

chronic inflammation. In addition, fibrous tissue appeared devoid of elastic fibers.

**Patient 4.** Lung section from a man aged 51–60 years with interstitial lung disease and extensive emphysema revealed patchy interstitial sub-pleural fibrosis with focal honeycombing as well as extensive emphysema.

**Patient 5.** A man aged 51–60 years admitted with tension pneumothorax underwent thoracoscopic excision of a giant bulla. Lung section showed emphysematous lung with multiple bullae.

**Patient 6.** A woman aged 51–60 years was evaluated for right lung nodule. She had been treated for colon cancer in the past. She was being treated for hypertension and there was a family history of lung cancer. The lung section revealed benign emphysematous lung parenchyma with focal intra-alveolar histiocytes.

**Patient 7.** A woman aged 51–60 years with COPD, hypothyroidism, and diabetes was admitted with acute respiratory difficulties and hypoxemia. Estimated RVSP was 52 mmHg. Despite intensive treatment the patient died. The lung section revealed intra-alveolar histiocytic infiltrate with sloughed alveolar lining and marked pulmonary artery intimal fibrosis. There was no evidence of cancer or acute inflammation.

**Patient 8.** A man aged 71–80 years with right lung traumatic entrapment, coronary artery disease (CAD; left main coronary artery obstruction), sleep apnea, and emphysema had had bacterial endocarditis in the past. Lung biopsy revealed fibrosing interstitial pneumonia, emphysema, septal fibrosis and focal osseous fatty metaplasia of visceral pleura, and medial hypertrophy of small pulmonary arteries.

**Patient 9.** A woman aged 71–80 years with CAD (required stent procedure), obesity, and abdominal aneurysm (repaired) was treated for retroperitoneal abscess. The RVSP was 52 mmHg. Lung section showed lung parenchyma with emphysematous changes, congestion, and hemorrhage.

### Chemicals and antibodies

All chemicals were purchased from Sigma Aldrich (St. Louis, MO, USA). Antibodies: cav-1 (sc-894), PTEN (sc-7974), HSP90 (sc-13119), and gp130 (sc-656) were bought from Santa Cruz Laboratories, CA, USA; eNOS (610296) and STAT3 (610189) were obtained from BD Transduction Laboratories (Palo Alto, CA, USA); Glut1 (ab15309) was obtained from Abcam laboratories, PY-STAT3 (9145) from Cell Signaling (Beverly, MA, USA), vWF(A0082) from Dako Cytomation (Carpinteria, CA, USA), and  $\beta$ -actin (A5441) from Sigma Aldrich.

### Protein extraction and western blot analysis

Western blot analysis was carried out as previously described.<sup>12</sup> Briefly, the lung tissue was homogenized in a buffer containing 0.1 M PBS (pH 7.4), 0.5% sodium deoxycholate, 1% Igepal, 0.1% SDS, 10  $\mu$ L/mL phenylmethylsulfonic fluoride (PMSF; 10 mg dissolved in 1 mL of isopropanol), 25  $\mu$ g/mL aprotinin, and 25  $\mu$ g/mL leupeptin. PMSF (10  $\mu$ L/mL) and phosphatase Inhibitor Cocktail 1 (10  $\mu$ L/mL; Sigma) were added to homogenates placed on ice for 30 min and centrifuged at 14,000 rpm for 20 min at 4 °C. A total of 50 or 100  $\mu$ g of protein from lung supernatants were loaded and separated on a 10% sodium SDS-polyacrylamide gel (Mini Protean-II, Bio-Rad) and transferred to nitrocellulose membrane (Hybond ECL, Amersham Life Science, MA, USA) using Semi Dry Transfer Cell (Bio-Rad). The membranes were blocked with 5% non-fat milk powder in Tris-Buffered-Saline with Tween buffer (TBST; 10 mM Tris-HCl, pH 7.4, 150 mM NaCl, 0.05% Tween 20) overnight at 4 °C. Membranes were then incubated with antibodies of interest; cav-1 (1:7000), gp130 (1:500), PTEN (1:400),  $\beta$ -catenin (1:400), Glut1 (1:400), PY-STAT3 (1:500), eNOS (1:500), and HSP90 (1:2000) for 1 h at room temperature, or overnight at 4 °C, according to the manufacturers' recommendations. The membranes were washed for 10 min  $\times$  3 with TBST and incubated with appropriate secondary antibody for 1 h at room temperature, then washed for 10 min  $\times$  3 with TBST buffer. The blots were reprobed with  $\beta$ -actin (1:10,000) or STAT3 (1:2000) as appropriate to assess the protein loading. The protein bands were visualized by chemiluminescence (ECL Western Blotting Analysis System, Amersham International). The relative expression of the proteins was quantified using densitometric scanning and is expressed as the ratio of protein of interest and  $\beta$ -actin or STAT3 as appropriate.

### Double immunofluorescence

Double immunofluorescence was carried out as described previously.<sup>30</sup> Briefly, lung sections were mounted on superfrost plus microscope slides (VWR Scientific, PA, USA) in preparation for immunofluorescence. Lung sections were deparaffinized in xylene (5 min  $\times$  2), rehydrated through a range of aqueous ethyl alcohol solution in H<sub>2</sub>O, and immersed in PBS for 5 min. Antigen retrieval was performed by incubating the sections in 10 mM citrate buffer, pH 6, in a microwave oven for 5 min. The slides were then incubated in blocking solution (5% normal donkey serum, 0.5% Triton in PBS) for 1 h at room temperature, followed by an overnight incubation at 4 °C with the primary antibody caveolin-1 $\alpha$  (1:100) in blocking solution. The next day the slides were washed with PBS for 10 min  $\times$  3 and incubated in Alexa 488 (donkey anti-rabbit, 1:300, green color, Molecular Probes) at room temperature in a dark place for 1 h followed by washing in PBS for 10 min  $\times$  3. For double staining, the sections were blocked again, as described earlier, and incubated

in the smooth muscle  $\alpha$ -actin antibody (1:15) overnight; the procedure was repeated using appropriate secondary antibody Alexa 594 (donkey anti-rabbit 1:200, or donkey anti-goat 1:200, red color, Molecular Probes). The sections were examined with a laser scanning confocal fluorescence microscope (MRC 1000, Bio-Rad). The negative controls were run in the absence of primary antibodies. In addition, double immunofluorescence study using vWF and smooth muscle  $\alpha$ -actin was performed on the lung sections.

### Statistical analysis

The data are expressed as means  $\pm$  SEM. For statistical analysis, we used one-way analysis of variance followed by Scheffe's multiple comparison tests. Differences were considered statistically significant at  $P < 0.05$ .

## Results

### Hemodynamic data

**Rats.** A progressive increase in RVSP (Fig. 1a, left panel) and RVH (right panel) indicative of PH was observed beginning at one week of hypoxic exposure. Figure 1b depicts thickening of medial wall in the hypoxia groups.

**Calves.** Consistent with previous findings,<sup>29</sup> there is a significant increase in the mean pulmonary arterial pressure (mPAP) in neonatal calves exposed to hypoxia for two weeks (Fig. 2a). Figure 2b depicts thin-walled pulmonary arteries from normal calves. Figure 2c shows significant medial wall and adventitial thickening in arteries (74–86  $\mu$ m and 186–240  $\mu$ m) in hypoxic neonatal calves. Similarly, impressive medial thickening in smaller (83–98  $\mu$ m) and larger arteries (177–324  $\mu$ m) is observed in Brisket disease, as shown in Fig. 2d.

**Expression of cav-1 and vWF.** Western blot analysis did not reveal any differences in the expression of cav-1 in rat or in bovine hypoxia groups compared with the respective controls (Figs. 3a and 4a). To localize the expression of cav-1, we conducted double immunofluorescence studies using cav-1 and  $\alpha$ -actin antibodies. We observed cav-1 in the endothelial layer of both rats and neonatal calves exposed to hypoxia, unchanged from controls as shown in Figs. 3b and 4b. Lung sections from steers with Brisket disease also show well-preserved cav-1 expression in the intimal layer of the pulmonary arteries. There is a significant medial thickening, without any evidence of intimal disruption (Fig. 4c). The immunofluorescence study in Fig. 3c shows that the expression of vWF is not altered by hypoxia in rat pulmonary arteries.

**Expression of eNOS and HSP90.** Impaired bioavailability of NO is an important feature of PH. We examined the expression of eNOS and HSP90 in the lung tissue of rats and calves subjected to hypoxia. As shown in Fig. 5, hypoxia does not

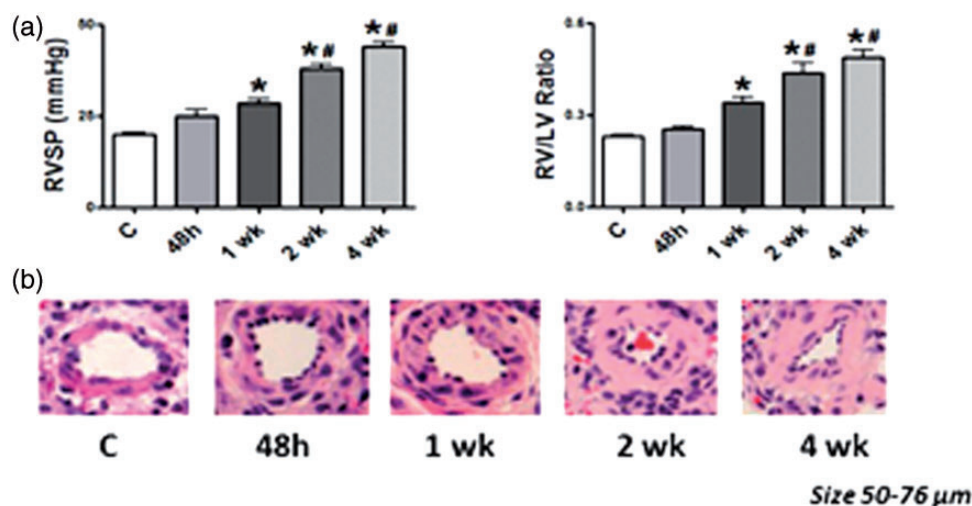


**Fig. 1.** (a) Significantly increased RVSP and right ventricular hypertrophy (RV/LV) at 1, 2, and 4 weeks of hypoxia in rats (n = 10–13). \*P < 0.05 vs. C (control), #P < 0.05 vs. 1 week. (b) The H&E figure depicts medial wall thickening in pulmonary arteries from hypoxia groups.

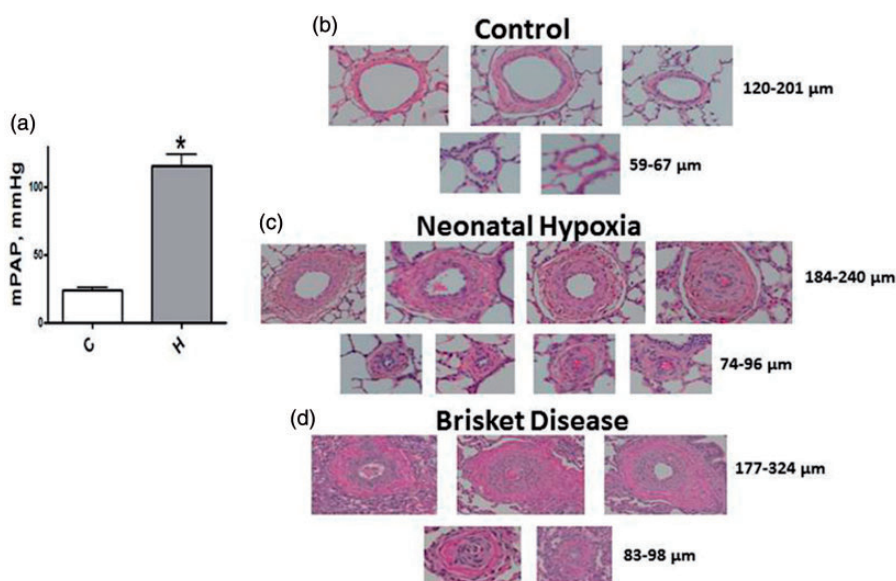


**Fig. 2.** (a) A significant increase in mPAP is seen in neonatal calves exposed to hypobaric hypoxia (n = 7–9). C, controls; H, hypoxic group. \*P < 0.05 vs. controls. (b) Thin walled pulmonary arteries of varying sizes from normal neonatal calves. (c) Arteries from neonatal hypoxia groups show significant medial thickness and lumens in some arteries appear obliterated. (d) Pulmonary arteries from steers with Brisket disease also show significant medial wall thickening and occlusion of some arteries.

alter the expression of eNOS or HSP90 in rats exposed to hypoxia (48 h, one, two, and four weeks) or in hypoxic neonatal calves.

**Loss of PTEN, PY-STAT3 activation, and increased Glut1 expression.** Western blots demonstrate a significant loss of PTEN at 48 h of hypoxia, which was persistent at four weeks (Fig. 6a). In parallel with the loss of PTEN, the activation of PY-STAT3 is observed at 48 h of hypoxia that is persistent at four weeks in rat lungs (Fig. 6b). There is a significantly increased expression of Glut1 in the lungs of

rats during hypoxia beginning at 48 h of hypoxia, coinciding with the loss of PTEN (Fig. 6c).

**Expression of gp130 and β-catenin.** Both cav-1 and PTEN are known to inhibit the activation of PY-STAT3 and the expression of β-catenin; since there is a loss of PTEN, we examined the expression of gp130 that activates PY-STAT3, and β-catenin expression in the lungs of rats and neonatal calves during hypoxia. Increased expression of gp130 and β-catenin are seen as early as within 48 h of hypoxia in rats, which remains persistent. Hypoxic neonatal calves

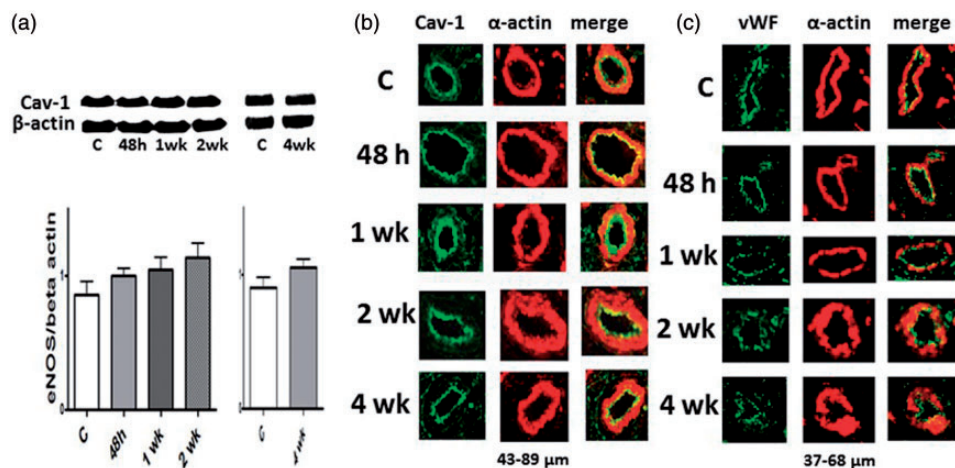


**Fig. 3.** (a) Representative western blots and bar graphs showing the expression of caveolin-1 in the rat lungs from the controls (C) and 48 h, and 1 and 2 weeks ( $n = 6$ ). Cav-1 expression in the hypoxia groups were not statistically different compared with the controls. (b) Immunofluorescence study showing the expression of cav-1 (green) and SM  $\alpha$ -actin (red) in the pulmonary arteries from the control and experimental groups. Hypoxia had no effect on the expression of cav-1 protein (western blot); the immunofluorescence study further confirms that there is no alteration in cav-1 expression during hypoxia; and the endothelial cav-1 is well-preserved. (c) Immunofluorescence study depicting the expression of vWF (green) and SM  $\alpha$ -actin (red) in the pulmonary arteries from the control and experimental groups. Hypoxia has not affected the expression of vWF.

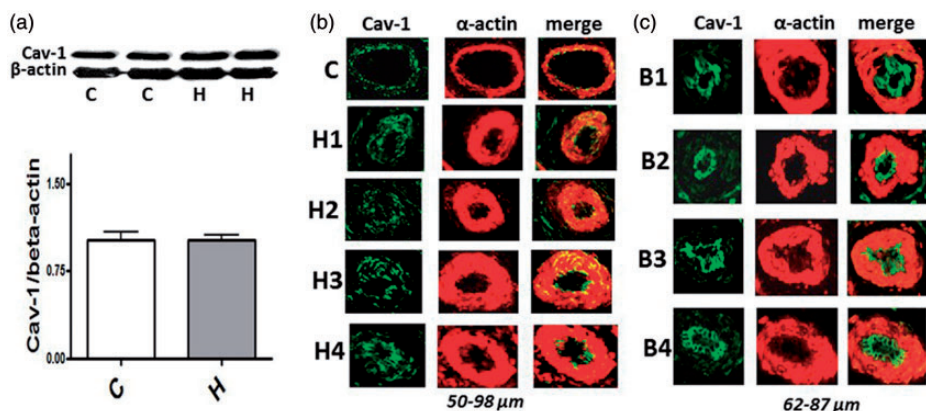


**Fig. 4.** (a) Representative western blots and bar graphs showing the expression of cav-1 in controls (C) and hypoxic (H) neonatal calves ( $n = 5-6$ ). (b) Immunofluorescence studies also did not show any alterations in the endothelial cav-1 expression in the neonatal hypoxia group (b, H1-H4) or in steers with Brisket disease (c, B1-B4). There is significant medial thickening. In H1, H2, and H3, few green speckles are seen in the medial layer. SMC normally has cav-1 which often is not well seen in immunofluorescence studies, but occasionally one can see a few speckles. It is important to note that the western blot does not reveal increased cav-1 expression in these bovine lung tissues. Cav-1 (green color) and SM  $\alpha$ -actin (red). C, control; H, hypoxia; H1-H4, hypoxia groups; B1-B4, Brisket disease groups.

also exhibit increased expression of gp130 and  $\beta$ -catenin (Fig. 7a and 7b).

### Chronic lung disease

Figure 8a (H&E stain) shows varying degrees of medial wall thickening in all patients except in Patient 4. Figure 8b shows cav-1 expression present in all arteries examined; however, the cav-1 staining appeared weak in several arteries, which may indicate partial loss of endothelial cav-1. The expression of vWF was not altered compared with the control (Fig. 8c).

### Discussion

The principal findings of the present study are, first, the expression of cav-1 in EC (immunofluorescence study) and in the lungs (western blot) in rats and neonatal calves is not altered by hypoxia. In addition, vWF expression is also well preserved in the EC in hypoxia-induced PH, indicating that the EC integrity is maintained. Second, the expression of eNOS and HSP90 is not reduced in rats or neonatal calves with hypoxia-induced PH. Third, a loss of PTEN and an increase in the expression of gp130,  $\beta$ -catenin, and Glut1 in the lungs of rats and neonatal calves are observed.

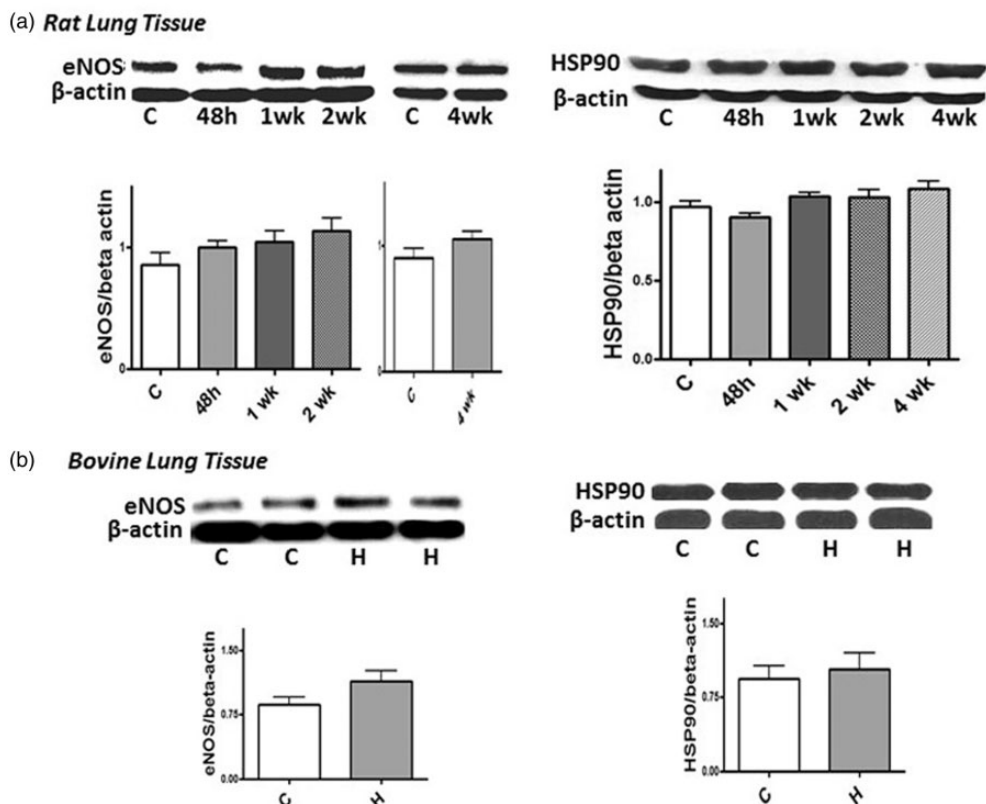


**Fig. 5.** Representative western blots and bar graphs showing the expression of eNOS ( $n = 6-8$ ) and HSP90 ( $n = 5-8$ ) in rat lungs from controls and after 48 h, and 1, 2, and 4 weeks of hypoxia (a). (b) The expression of eNOS (48 h, 1 and 2 weeks,  $n = 7-9$ ) and HSP90 ( $n = 8$ ) in the control and hypoxic bovine lungs. As a loading control,  $\beta$ -actin was used. The expression of eNOS or HSP90 was not altered during hypoxia in rats or calves ( $P = NS$ ).

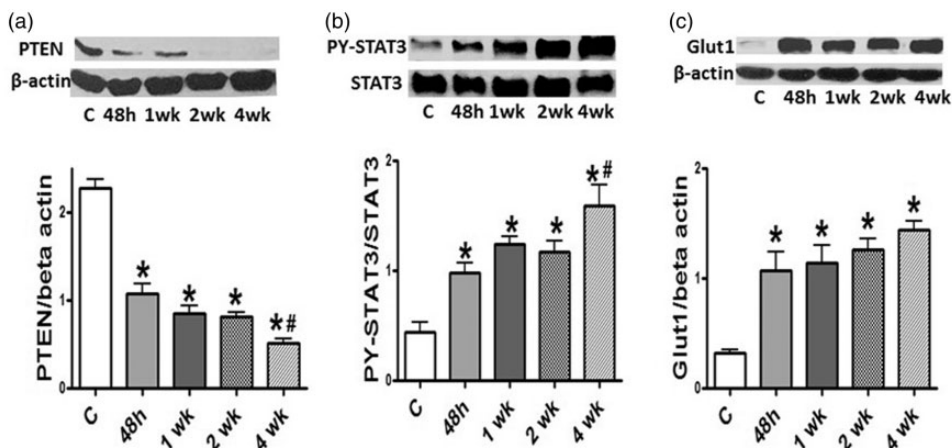


**Fig. 6.** (a) A representative western blot and a bar graph depicting the expression of PTEN in the controls and 48 h, and 1, 2, and 4 weeks of hypoxia ( $n = 3-7$ ). Significant reduction in PTEN expression is present at 48 h, and 1 and 2 weeks of hypoxia, and a further reduction at 4 weeks. (b) A western blot and bar graph depicting the expression of PY-STAT3 and STAT3 in the controls and 48 h, 1, 2, and 4 weeks of hypoxia ( $n = 5-7$ ). Significant activation of PY-STAT3 is present at 48 h, and 1 and 2 weeks of hypoxia. There is a further increase in PY-STAT3 activation at 4 weeks of hypoxia. (c) A representative western blot and a bar graph depicting the expression of Glut1 in controls and 48 h, and 1, 2, and 4 weeks of hypoxia ( $n = 4-5$ ). Significant increase in the expression of Glut1 is present at 48 h, 1, 2, and 4 weeks of hypoxia. \* $P < 0.05$  vs. controls (C), # $P < 0.05$  vs. 48 h group.

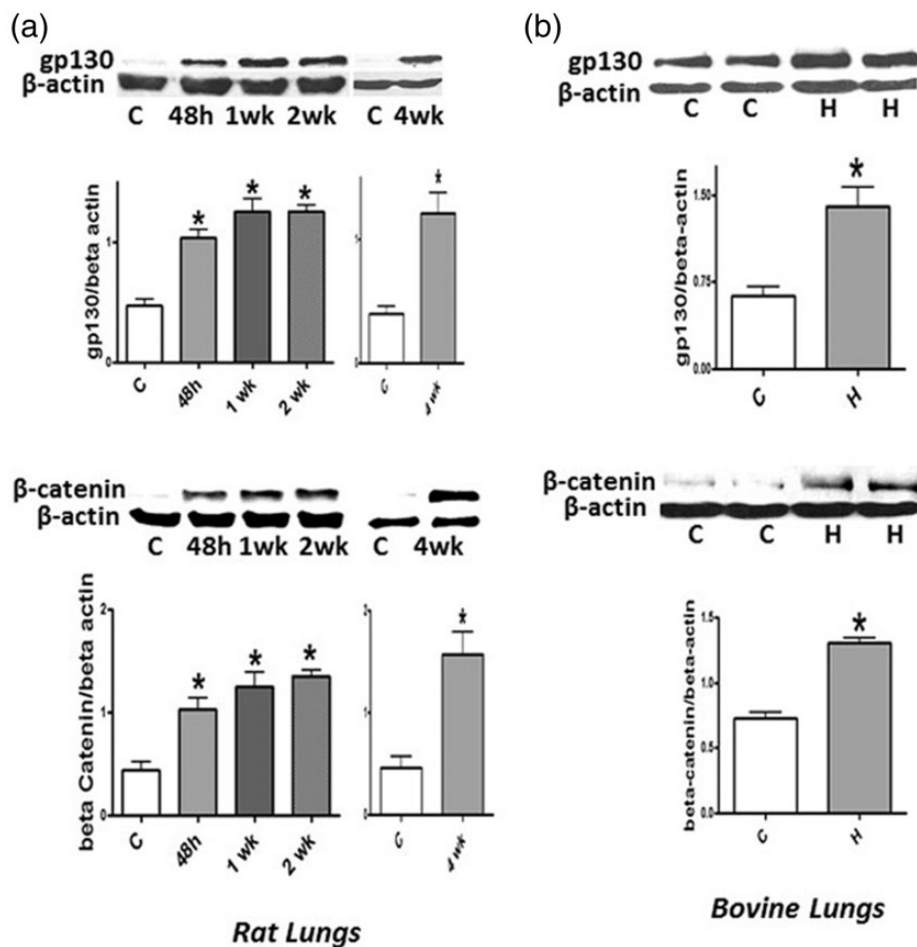


**Fig. 7.** Representative western blots and bar graphs showing the expression of gp130 ( $n=5-6$ ) and  $\beta$ -catenin ( $n=5-6$ ) in controls and 48 h, and 1, 2, and 4 weeks of hypoxia in rats (a). (b) gp130 ( $n=4-5$ ) and  $\beta$ -catenin ( $n=5-6$ ) in controls (C) and neonatal hypoxia calves (H). There is a significant increase in the expression of gp130 and  $\beta$ -catenin both in hypoxic rats and calves. \* $P < 0.05$  vs. controls (C).

These alterations are seen in rats within 48 h of hypoxic exposure. Fourth, the activation of PY-STAT3 in rat lungs is seen within 48 h of hypoxic exposure. The loss of PTEN and increased expression of gp130, the activation of PY-STAT3, and increased  $\beta$ -catenin and Glut1, despite the presence of cav-1, indicate the loss of normal cav-1 function. And, finally, the lung sections from patients with chronic lung disease showed the presence of endothelial cav-1, albeit slightly scant in some cases. The vWF expression was not altered.

Impaired nitric oxide-mediated endothelium-dependent pulmonary vascular relaxation responses have been reported in PAH associated with congenital heart defect, and in the MCT and hypoxia models of PH.<sup>3,31,32</sup> In the MCT model of PH, in addition to the progressive loss of endothelial cav-1, a significant reduction in the expression of HSP90 (2 weeks after MCT) and eNOS (three weeks after MCT) have been reported.<sup>8</sup> However, unlike the MCT model, hypoxia does not alter the expression of cav-1, eNOS, or HSP90. Cav-1 and eNOS have a dynamic relationship, the interaction between cav-1 and eNOS results in the inhibition

of eNOS function; and the interaction between HSP90 and eNOS results in dissociation of eNOS from cav-1, restoring eNOS function. Importantly, in response to  $\text{Ca}^{2+}$  agonists, eNOS dissociates from cav-1 and binds to HSP90.  $\text{Ca}^{2+}$ -activated calmodulin further aids in recruitment of HSP90, thus facilitating the release of eNOS from cav-1.<sup>33</sup> Consistent with our observation, recent studies have shown that during hypoxia, cav-1 and eNOS form a tight complex in vivo and in vitro, resulting in their dysfunction.<sup>10,34</sup> Furthermore, hypoxia has also been shown to disrupt eNOS/HSP90 binding.<sup>35</sup> Thus, the hypoxia-induced cav-1/eNOS complex formation may in part be responsible for the disruption of HSP90/eNOS binding leading to impaired vascular relaxation. Statins have been shown to inhibit hypoxia-induced abnormal coupling of eNOS and cav-1, restoring eNOS function, and attenuating hypoxia-induced PH.<sup>36</sup> Hypoxia has been shown to alter the physical state of EC, lipid composition, and plasma membrane function. These alterations are reversible on return to normoxic state.<sup>37</sup> Interestingly, hypoxia also reduces caveolar density.<sup>38</sup> Cav-1 and eNOS have been shown to form a tight

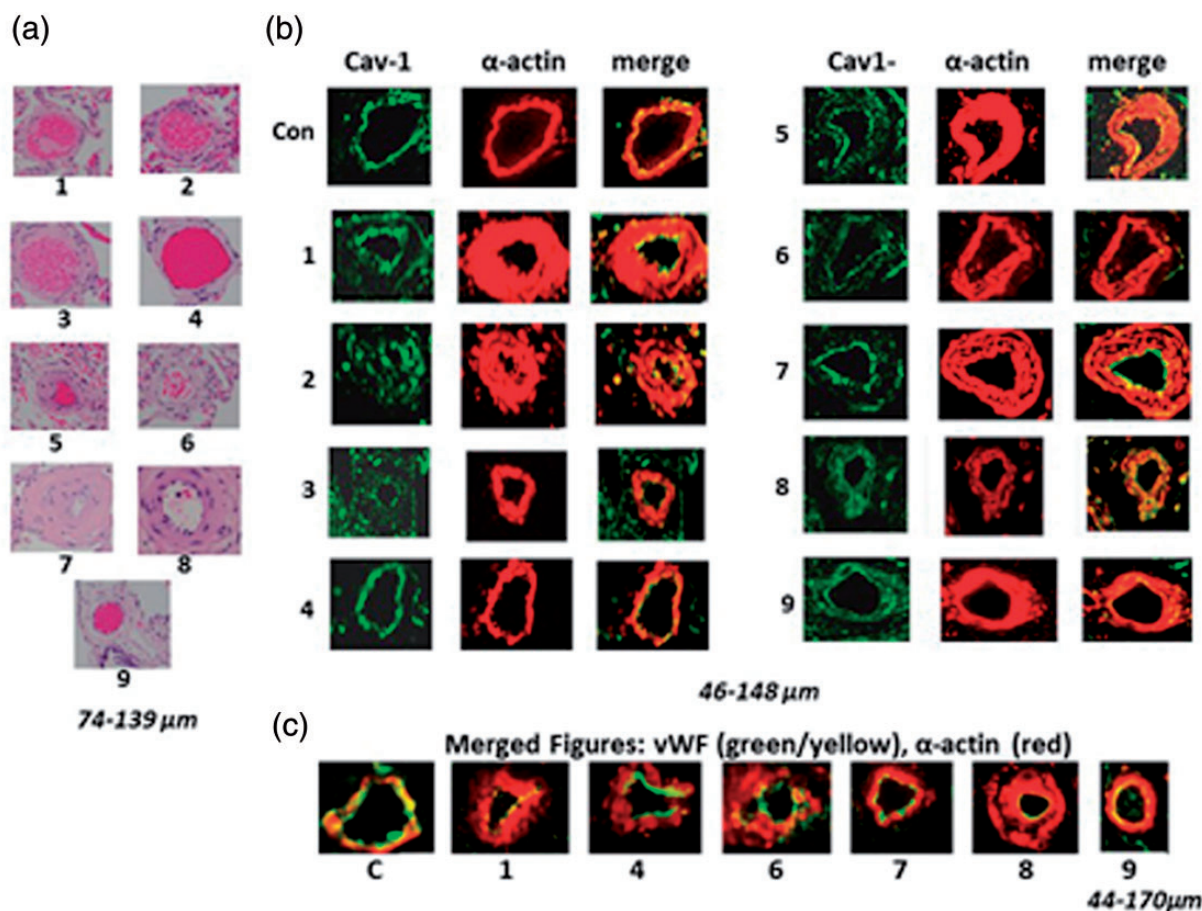


**Fig. 8.** (a) H&E staining of the pulmonary arteries from Patients 1–9. Most arteries show varying degrees of medial thickening except Patient 4, despite extensive emphysema. (b) Immunofluorescence study depicting the expression of cav-1 (green) and smooth muscle  $\alpha$ -actin (red) in pulmonary arteries. The control artery (Con) and the arteries from patients with chronic lung display the presence of endothelial cav-1. (c) Representative immunofluorescence study showing the expression of vWF (yellow/green) and smooth muscle  $\alpha$ -actin (red) as merged figures. There is no loss of vWF in the group of patients with the lung diseases we studied.

complex in bovine EC when exposed to hypoxia; and the complex appeared to be in the cytosol.<sup>34</sup> It is possible that the hypoxia-induced eNOS/cav-1 complex has an effect on the caveolar density. However, further studies are required to establish the mechanism of reduced caveolar density during hypoxia-induced PH.

Both STAT3 and Wnt/ $\beta$ -catenin are essential for embryonic development of multiple organs, cell proliferation, and growth. Upon activation,  $\beta$ -catenin, a transcription factor of the Wnt pathway, accumulates in the nucleus and complexes with T-cell factor/lymphoid enhancing factor (TCF/LEF) to activate gene transcription.<sup>39</sup> Recent studies have shown that not only PY-STAT3 but also  $\beta$ -catenin plays a critical role in vascular smooth muscle proliferation and neointima formation in carotid artery balloon injury model.<sup>40</sup> PY-STAT3, a downstream effector of IL-6 activated by its binding to gp130, a plasma membrane receptor, plays a critical role in cell growth, inhibition of apoptosis, survival, and in immune function and inflammation. Activated STAT3 upregulates several genes involved in cell proliferation and confers

resistance to apoptosis.<sup>41,42</sup> Importantly, rescue of cav-1 has been shown to attenuate PY-STAT3 activation in the MCT model of PH.<sup>12</sup> Furthermore, PY-STAT3 activation has been observed in pulmonary EC from patients with idiopathic PAH; the reduction of PY-STAT3 in these EC in cell culture studies resulted in the inhibition of cell proliferation.<sup>13</sup> Activation of Wnt pathway inhibits glycogen synthase kinase 3 $\beta$ -dependent phosphorylation and degradation of  $\beta$ -catenin. The role of PY-STAT3 and Wnt/ $\beta$ -catenin pathway is well established in several forms of cancer.<sup>43</sup> Recent studies have shown that PY-STAT3 and also  $\beta$ -catenin play a critical role in vascular smooth muscle proliferation and neointima formation.<sup>40,44</sup> In the present study, the upregulation of  $\beta$ -catenin occurred within 48 h of hypoxia in rats, concomitant with the activation of PY-STAT3. Increased  $\beta$ -catenin is also observed in neonatal calves with hypoxia-induced PH. Thus, it is likely that in hypoxia-induced PH, STAT3, and  $\beta$ -catenin may have synergistic effects further supporting a role for  $\beta$ -catenin, in addition to PY-STAT3 in PH.

Despite the presence of cav-1 expression in the EC during hypoxia-induced PH, there is a significant loss of PTEN as early as 48 h of hypoxia, before the onset of PH. Interestingly, overexpression of cav-1 restores PTEN expression in idiopathic lung fibrosis.<sup>20</sup> It is worth noting here that cav-1 expression is necessary for the membrane localization of PTEN. PTEN is known not only to negatively regulate STAT3 activation,<sup>22,23</sup> but also to antagonize nuclear accumulation of  $\beta$ -catenin. In some forms of cancer, the WNT/ $\beta$ -catenin pathway is reported to promote aerobic glycolysis and cell proliferation depending on the status of PTEN. Elevated PTEN levels promote oxidative phosphorylation, reduce glycolysis, and decrease cell proliferation.<sup>45,46</sup> Our studies further show that increased levels of PY-STAT3 and  $\beta$ -catenin in hypoxia-induced PH coincide with the loss of PTEN. In addition, loss of PTEN is associated with increased expression of Glut1 as shown in Fig. 6. This is consistent with previous studies showing significantly decreased PTEN messenger RNA and concomitantly increased Glut1 expression in pulmonary vascular adventitial fibroblasts from hypoxia-exposed neonatal calves and patients with idiopathic PAH.<sup>27,47</sup> It is likely that the hypoxia-induced dysfunction of cav-1 may, in part, be responsible for the loss of PTEN leading to the increased expression of Glut1,  $\beta$ -catenin, and the activation of PY-STAT3. Thus, the dysfunction of cav-1 coupled with the loss of PTEN may play a major role in the pathogenesis of hypoxia-induced PH.

In the human lung sections we examined, we did not observe a loss of cav-1 or vWF, indicating that EC were not disrupted. Moderate PH was documented in only two cases. Endothelial dysfunction has been observed in mild cases of COPD and the loss of endothelium-dependent relaxation in the pulmonary vasculature correlates with the severity of the disease.<sup>6,48</sup> Interestingly, the outflow obstruction in COPD results from inflammatory processes affecting airways, lung parenchyma, and pulmonary vasculature. PH in COPD has been shown to develop independently of underlying parenchymal destruction and loss of lung vessels.<sup>49,50</sup> Importantly, Huber et al.<sup>51</sup> have shown loss of endothelial cav-1 accompanied by enhanced expression of cav-1 in SMC in COPD associated with PH. In their series, COPD without PH had preserved endothelial cav-1. Furthermore, severe pulmonary arterial lesions such as plexiform and angiomatoid lesions have been documented in explanted lungs after transplantation in COPD associated with severe PH. These lesions were similar to those seen in idiopathic PAH.<sup>52</sup> We have previously shown that infants with respiratory distress syndrome, despite significantly elevated PAP and significant medial thickening, exhibit well preserved endothelial cav-1 in pulmonary arteries, without any evidence of EC disruption or enhanced expression of cav-1 in SMC. In contrast, loss of endothelial cav-1, disruption/loss of EC coupled with enhanced expression of cav-1 in SMC was seen in infants with bronchopulmonary dysplasia and associated inflammation.<sup>53</sup> In human PAH and the

MCT model, progressive endothelial cav-1 loss is followed by a loss of vWF indicative of extensive EC damage. These changes precede enhanced cav-1 expression in SMC.<sup>30,53</sup> The MCT + hypoxia model and human PAH have been reported to show progressive disruption and loss of endothelial cav-1 leading to extensive EC damage and a subsequent enhanced expression of cav-1 in SMC, followed by neointima formation.<sup>54,55</sup> Importantly, isolated SMC from idiopathic PAH patients revealed increased cav-1 expression, associated with increased capacitative  $\text{Ca}^{2+}$  entry and DNA synthesis, which could be reverted by silencing cav-1.<sup>55</sup> Thus, the loss of endothelial cav-1 and EC disruption may have a worsening effect on the progression of PH.

In summary, endothelial cav-1 and vWF are well preserved during hypoxia-induced PH, indicating that the EC integrity is not disrupted. However, despite the presence of endothelial cav-1, the expression of PTEN is significantly reduced in the lungs. Since PTEN requires cav-1 for its membrane localization, the loss of PTEN is suggestive of cav-1 dysfunction. In addition, hypoxia-induced PH is accompanied by the activation of PY-STAT3 and increased  $\beta$ -catenin and glut1 expression. Both cav-1 and PTEN are known to inhibit the activation of PY-STAT3 and the increased expression of  $\beta$ -catenin and glut1. Thus, the cav-1 dysfunction and accompanying loss of PTEN may have an important role in hypoxia-induced PH.

### Conflict of interest

The author(s) declare that there is no conflict of interest.

### Funding

This work in part was supported in part by CMREF awarded to RM, and P01HL014985 (NHLBI), R01HL114887 (NHLBI) and PR140977 (DoD) awarded to KS.

### References

1. Rabinovitch M, Gamble W, Nadas AS, et al. Rat pulmonary circulation after chronic hypoxia: hemodynamic and structural features. *Am J Physiol* 1979; 236: H818–H827.
2. Drexler ES, Bischoff JE, Slifka AJ, et al. Stiffening of the extrapulmonary arteries from rats in chronic hypoxic pulmonary hypertension. *J Res Natl Inst Stand Technol* 2008; 113: 239–249.
3. Adnot S, Raffestin B, Eddahibi S, et al. Loss of endothelium-dependent relaxant activity in the pulmonary circulation of rats exposed to chronic hypoxia. *J Clin Invest* 1991; 87: 155–162.
4. Murata T, Yamawaki H, Hori M, et al. Hypoxia impairs endothelium-dependent relaxation in organ cultured pulmonary artery. *Eur J Pharmacol* 2001; 421: 45–53.
5. Dinh-Xuan AT, Higenbottam TW, Clelland CA, et al. Impairment of endothelium-dependent pulmonary-artery relaxation in chronic obstructive lung disease. *N Eng J Med* 1991; 324: 1539–1547.
6. Peinado VI, Barbera JA, Ramirez J, et al. Endothelial dysfunction in pulmonary arteries of patients with mild COPD. *Am J Physiol* 1998; 274: L908–L913.

7. Mathew R. Pathogenesis of pulmonary hypertension: a case for caveolin-1 and cell membrane integrity. *Am J Physiol Heart Circ Physiol* 2014; 306: H15–H25.
8. Huang J, Wolk JH, Gewitz MH, et al. Progressive endothelial cell damage in an inflammatory model of pulmonary hypertension. *Exp Lung Res* 2010; 36: 57–66.
9. Mathew R, Huang J, Katta US, et al. Immunosuppressant-induced endothelial damage and pulmonary arterial hypertension. *J Pediatr Hematol Oncol* 2011; 33: 55–58.
10. Murata T, Sato K, Hori M, et al. Decreased endothelial nitric-oxide synthase (eNOS) activity resulting from abnormal interaction between eNOS and its regulatory proteins in hypoxia-induced pulmonary hypertension. *J Biol Chem* 2002; 277: 44085–44092.
11. Paffett ML, Naik JS, Riddle MA, et al. Altered membrane lipid domains limit pulmonary endothelial calcium entry following chronic hypoxia. *Am J Physiol Heart Circ Physiol* 2011; 301: H1331–H1340.
12. Huang J, Kaminski PM, Edwards JG, et al. Pyrrolidine dithiocarbamate restores endothelial cell membrane integrity and attenuates monocrotaline-induced pulmonary artery hypertension. *Am J Physiol Lung Cell Mol Physiol* 2008; 294: L1250–L1259.
13. Masri FA, Xu W, Comhair SA, et al. Hyperproliferative apoptosis-resistant endothelial cells in idiopathic pulmonary arterial hypertension. *Am J Physiol Lung Cell Mol Physiol* 2007; 293: L548–L554.
14. Jasmin JF, Mercier I, Sotgia F, et al. SOCS protein and caveolin-1 as negative regulators of endocrine signaling. *Trends Endocrinol Metabol* 2006; 17: 150–158.
15. Rai PR, Cool CD, King JA, et al. The cancer paradigm of severe pulmonary arterial hypertension. *Am J Respir Crit Care Med* 2008; 178: 558–564.
16. Laumanns IP, Fink L, Wilhelm J, et al. The noncanonical WNT pathway is operative in idiopathic pulmonary arterial hypertension. *Am J Respir Cell Mol Biol* 2009; 40: 683–691.
17. Galbiati F, Volonte D, Brown AM, et al. Caveolin-1 expression inhibits Wnt/ $\beta$ -catenin/Lef-1 signaling by recruiting  $\beta$ -catenin to caveolae membrane domains. *J Biol Chem* 2000; 275: 23368–23377.
18. Ravi Y, Selvendiran K, Meduru S, et al. Dysregulation of PTEN in cardiopulmonary vascular remodeling induced by pulmonary hypertension. *Cell Biochem Biophys* 2013; 67: 363–372.
19. Caselli A, Mazzinghi B, Camici G, et al. Some protein tyrosine phosphatases target in part to lipid rafts and interact with caveolin-1. *Biochem Biophys Res Commun* 2002; 296: 692–697.
20. Xia H, Khalil W, Kahm J, et al. Pathologic caveolin-1 regulation of PTEN in idiopathic pulmonary fibrosis. *Am J Pathol* 2010; 176: 2626–2637.
21. Persad A, Venkateswaran G, Hao L, et al. Active  $\beta$ -catenin is regulated by the PTEN/PI3 kinase pathway: a role for protein phosphatase PP2A. *Genes & Cancer* 2016; 7: 368–382.
22. Lin HY and Palmieri C. Is STAT3 and PTEN expression altered in canine prostate cancer? *J Comp Path* 2016; 155: 185–189.
23. Sun S and Steinberg BM. PTEN is a negative regulator of STAT3 activation in human papillomavirus-infected cells. *J Gen Virol* 2002; 83: 1651–1658.
24. Morani F, Phadngam S, Follo C, et al. PTEN regulates plasma membrane expression of glucose transporter 1 and glucose uptake in thyroid cancer cells. *J Mol Endocrinol* 2014; 53: 247–258.
25. Phadngam S, Castiglioni A, Ferraresi A, et al. PTEN dephosphorylates AKT to prevent the expression of GLUT1 on plasma membrane and to limit glucose consumption in cancer cells. *Oncotarget* 2016; 7: 84999–85020.
26. Sakyo T and Kitagawa T. Differential localization of glucose transporter isoforms in non-polarized mammalian cells: distribution of GLUT1 but not GLUT3 to detergent-resistant membrane domains. *Biochim Biophys Acta* 2002; 1567: 165–175.
27. Yao G, Zhang Y, Wang D, et al. GDM-Induced macrosomia is reversed by cav-1 via AMPK-mediated fatty acid transport and GLUT1-mediated glucose transport in placenta. *PLoS One* 2017; 12: e0170490.
28. Newman JH, Holt TN, Hedges LK, et al. High-altitude pulmonary hypertension in cattle (brisket disease): Candidate genes and gene expression profiling of peripheral blood mononuclear cells. *Pulm Circ* 2011; 1: 462–469.
29. Stenmark KR, Fasules J, Hyde DM, et al. Severe pulmonary hypertension and arterial adventitial changes in newborn calves at 4,300 m. *J Appl Physiol (1985)* 1987; 62: 821–830.
30. Huang J, Wolk JH, Gewitz MH, et al. Caveolin-1 expression during the progression of pulmonary hypertension. *Exp Biol Med (Maywood)* 2012; 237: 956–965.
31. Celermajer DS, Cullen S and Deanfield JE. Impairment of endothelium-dependent pulmonary artery relaxation in children with congenital heart disease and abnormal pulmonary hemodynamics. *Circulation* 1993; 87: 440–446.
32. Mathew R, Zeballos GA, Tun H, et al. Role of nitric oxide and endothelin-1 in monocrotaline-induced pulmonary hypertension in rats. *Cardiovasc Res* 1995; 30: 739–746.
33. Gratton JP, Fontana J, O'Connor DS, et al. Reconstitution of an endothelial nitric-oxide synthase (eNOS), hsp90, and caveolin-1 complex in vitro. Evidence that hsp90 facilitates calmodulin stimulated displacement of eNOS from caveolin-1. *J Biol Chem* 2000; 275: 22268–22272.
34. Mathew R. Cell-specific dual role of caveolin-1 in pulmonary hypertension. *Pulm Med* 2011; 2011: 573432.
35. Fike CD, Pfister SL, Slaughter JC, et al. Protein complex formation with heat shock protein 90 in chronic hypoxia-induced pulmonary hypertension in newborn piglets. *Am J Physiol* 2010; 299: H1190–H1204.
36. Murata T, Kinoshita K, Hori M, et al. Statin protects endothelial nitric oxide synthase activity in hypoxia-induced pulmonary hypertension. *Atheroscler Thromb Vasc Biol* 2005; 25: 2335–2342.
37. Block ER, Patel JM and Edwards D. Mechanism of hypoxic injury to pulmonary artery endothelial cell plasma membranes. *Am J Physiol* 1989; 257: C223–C231.
38. Botto L, Beretta E, Daffara R, et al. Biochemical and morphological changes in endothelial cells in response to hypoxic interstitial edema. *Respir Res* 2006; 7: 7.
39. Logan CY and Lai WC. The Wnt signaling pathway in development and disease. *Annu Rev Cell Dev Biol* 2004; 20: 781–810.
40. Wang X, Xiao Y, Mou Y, et al. A role for  $\beta$ -catenin/T-cell factor signaling cascade in vascular remodeling. *Circ Res* 2002; 90: 340–347.
41. Bromberg J. STAT proteins and oncogenesis. *J Clin Invest* 2002; 109: 1139–1142.

42. Darnell JE Jr. STATs and gene regulation. *Science* 1997; 277: 1630–1635.
43. Giles RH, van Es JH and Clevers H. Caught up in a Wnt storm: Wnt signaling in cancer. *Biochim Biophys Acta* 2003; 1653: 1–24.
44. Shibata R, Kai H, Seki Y, et al. Inhibition of STAT3 prevents neointima formation by inhibiting proliferation and promoting apoptosis of neointimal smooth muscle cells. *Hum Gene Ther* 2003; 14: 601–610.
45. Brown K, Yang P, Salvador D, et al. WNT/ $\beta$ -catenin signaling regulates mitochondrial activity to alter the oncogenic potential of melanoma in a PTEN-dependent manner. *Oncogene* 2017; 36: 3119–3136.
46. Garcia-Cao I, Song MS, Hobbs RM, et al. Systemic elevation of PTEN induces a tumor-suppressive metabolic state. *Cell* 2012; 149: 49–62.
47. Wang D, Zhang H, Li M, et al. MicroRNA-124 controls the proliferative, migratory, and inflammatory phenotype of pulmonary vascular fibroblasts. *Circ Res* 2014; 114: 67–78.
48. Polverino F, Celli BR and Owen CA. COPD as an endothelial disorder: endothelial injury linking lesions in the lungs and other organs? (2017 Grover Conference Series). *Pulm Circ* 2018; 8: 1–18.
49. Blanco I, Piccari L and Barberà JA. Pulmonary vasculature in COPD: The silent component. *Respirology* 2016; 21: 984–994.
50. Sakao S, Voelkel NF and Tatsumi K. The vascular bed in COPD: pulmonary hypertension and pulmonary vascular alterations. *Eur Respir Rev* 2014; 23: 350–355.
51. Huber LC, Soltermann A, Fischler M, et al. Caveolin-1 expression and hemodynamics in COPD patients. *Open Respir Med J* 2009; 3: 73–78.
52. Carlsen J, Hasseriis Andersen K, Boesgaard S, et al. Pulmonary arterial lesions in explanted lungs after transplantation correlate with severity of pulmonary hypertension in chronic obstructive pulmonary disease. *J Heart Lung Transplant* 2013; 32: 347–354.
53. Dereddy N, Huang J, Erb M, et al. Associated inflammation or increased flow-mediated shear stress, but not pressure alone, disrupts endothelial caveolin-1 in infants with pulmonary hypertension. *Pulm Circ* 2012; 2: 492–500.
54. Huang J, Wolk JH, Gewitz MH, et al. Enhanced caveolin-1 expression in smooth muscle cells: Possible prelude to neointima formation. *World J Cardiol* 2015; 7: 671–684.
55. Patel HH, Zhang S, Murray F, et al. Increased smooth muscle cell expression of caveolin-1 and caveolae contribute to the pathophysiology of idiopathic pulmonary arterial hypertension. *FASEB J* 2007; 21: 2970–2979.